Journal of Cellular Biochemistry

Activated α2-Macroglobulin Induces Mesenchymal Cellular Migration of Raw264.7 Cells Through Low-Density Lipoprotein Receptor-Related Protein 1

Journal:	*Journal of Cellular Biochemistry*
Manuscript ID	Draft
Wiley - Manuscript type:	Research Article
Date Submitted by the Author:	n/a
Complete List of Authors:	Ferrer, Dario; Facultad de Ciencias Químicas, Universidad Nacional de Córdoba, Bioquímica Clínica (CIBICI-CONICET) Actis Dato, Virginia; Facultad de Ciencias Químicas, Universidad Nacional de Córdoba, Bioquímica Clínica (CIBICI-CONICET) Jaldin Fincati, Javier; Facultad de Ciencias Químicas, Universidad Nacional de Córdoba, Bioquímica Clínica (CIBICI-CONICET); The Hospital for Sick Children, Cell Biology Program, Research Institute Lorenc, Valeria; Facultad de Ciencias Químicas, Universidad Nacional de Córdoba, Bioquímica Clínica (CIBICI-CONICET); The Wilmer Eye Institute, Johns Hopkins University Sánchez, María; Facultad de Ciencias Químicas, Universidad Nacional de Córdoba, Bioquímica Clínica (CIBICI-CONICET) Chiabrando, Gustavo; Facultad de Ciencias Químicas, Universidad Nacional de Córdoba, Bioquímica Clínica (CIBICI-CONICET)
Keywords:	α-macroglobulins, endocytosis, LDL receptors, migration

Activated α_2-Macroglobulin Induces Mesenchymal Cellular Migration of Raw264.7 Cells Through Low-Density Lipoprotein Receptor-Related Protein 1

Darío G. Ferrer[*], Virginia Actis Dato[*], Javier R. Jaldín Fincati*[1], Valeria E. Lorenc*[2], María C. Sánchez[*], Gustavo A. Chiabrando*[§]

*Centro de Investigaciones en Bioquímica Clínica e Inmunología (CIBICI), Departamento de Bioquímica Clínica, Facultad de Ciencias Químicas, Universidad Nacional de Córdoba, Haya de la Torre y Medina Allende, Ciudad Universitaria (5000), Córdoba, Argentina

[1]Present address: Cell Biology Program, Research Institute The Hospital for Sick Children, Toronto, Ontario, Canada

[2]Present address: The Wilmer Eye Institute, Johns Hopkins University, Baltimore, Maryland, USA

[§]**Corresponding author**: Dr. Gustavo A. Chiabrando, CIBICI-CONICET, Haya de la Torre y Medina Allende, Ciudad Universitaria (5000), Córdoba, Argentina. Tel: +54 351 4334264 Ext.: 3431; Fax: +54 351 4333048; E-mail: gustavo@fcq.unc.edu.ar

Running head: The α_2M/LRP1 induces mesenchymal migration

Key words: α-macroglobulins; endocytosis; LDL receptors; migration

Total number of text figures: Five figures and four supplementary figures

Grants: Secretaría de Ciencia y Tecnología de la Universidad Nacional de Córdoba (SECyTUNC) grants 124/13 and 162/12. Fondo para la Investigación Científica y Tecnológica (FONCyT): Préstamo BID Proyecto de Investigación en Ciencia y Tecnología (PICT) grant 2012-2607. Consejo Nacional de Investigaciones Científicas y Técnicas (CONICET) Proyecto de Investigación Plurianual (PIP) grant 11220110100775.

ABSTRACT

Distinct modes of cell migration contribute to diverse types of cell movements. The mesenchymal mode is characterized by a multistep cycle of membrane protrusion, the formation of focal adhesion, and the stabilization at the leading edge associated with the degradation of extracellular matrix (ECM) components and with regulated extracellular proteolysis. Both α_2-Macroglobulin (α_2M) and its receptor, low density lipoprotein receptor-related protein 1 (LRP1), play important roles in inflammatory processes, by controlling the extracellular activity of several proteases. The binding of the active form of α_2M (α_2M*) to LRP1 can also activate different signaling pathways in macrophages, inducing extracellular matrix metalloproteinase-9 (MMP-9) activation and cellular proliferation. In the present study, we investigated whether the α_2M*/LRP1 interaction induces cellular migration of the macrophage-derived cell line, Raw264.7. By using the wound-scratch migration assay and confocal microscopy, we demonstrate that α_2M* induces LRP1-mediated mesenchymal cellular migration, characterized by the production of enlarged cellular protrusions, MT1-MMP distribution to these leading edge protrusions, actin polymerization, focal adhesion formation, and increased intracellular LRP1/β1-integrin colocalization. Moreover, the α_2M*-stimulated cellular protrusions were fully blocked by the presence of calphostin-C. This indicates that the PKC activation is involved in the cellular motility of Raw264.7 cells. These findings could constitute a therapeutic target for inflammatory processes with deleterious consequences for human health, such as rheumatoid arthritis, atherosclerosis and cancer.

Alpha$_2$-Macroglobulin (α_2M) is a plasma protease inhibitor with broad specificity. Structurally, it is a tetrameric protein composed of two noncovalently associated dimers of disulfide-linked identical subunits (≈180 kDa). The α_2M structure is characterized by a proteolysis-sensitive bait sequence and an internal β-cysteinyl-γ-glutamyl thiol ester bond per subunit. The bait region is susceptible to cleavage by proteases, whereas thiol ester bonds are a target for nucleophilic attack by monoamines [Chu and Pizzo, 1994]. Consequently, α_2M undergoes a conformational change upon complex formation with proteases, and thus becomes an activated form, known as α_2M*. This activated form specifically binds to the receptor low-density lipoprotein (LDL) receptor-related protein 1 (LRP1), a member of the LDL receptor gene family. However, α_2M* only recognizes LRP1 among the LDL receptor members [Hussain et al., 1999]. Alpha$_2$M* is internalized by LRP1 through clathrin-dependent endocytosis and degraded in lysosomes, which is a protease debugging mechanism from extracellular space [Herz and Strickland, 2001]. In addition, the α_2M* binding to LRP1 activates different intracellular signaling pathways in Müller glial cells [Barcelona et al., 2011], Schwann cells [Mantuano et al., 2011], and macrophages [Bonacci et al., 2007; Caceres et al., 2010].

LRP1 is a cell surface glycoprotein synthesized as a precursor protein of 600 kDa. It is proteolytically cleaved by furin into two subunits: a large subunit of 515 kDa (LRP1-α), containing the extracellular binding domain, and one of 85 kDa (LRP1-β), which comprises membrane spanning and cytoplasmatic domains. These subunits are associated through noncovalent interactions [Herz and Strickland, 2001]. LRP1 is a typical scavenger receptor that interacts with and internalizes many different ligands in addition to α_2M*. However, these ligands do not compete with each other for binding to

the receptor, with the exception of the receptor-associated protein (RAP). RAP is a chaperon protein that binds to and blocks the binding of all known ligands to the receptor. After receptor-mediated endocytosis, certain ligands follow a lysosomal degradation pathway, such as α_2M* and RAP [Herz and Strickland, 2001], whereas others, such as apolipoprotein E (ApoE), are re-secreted following a non-degradation pathway [Laatsch et al., 2012]. However, regardless of the ligand interacting with LRP1, this receptor is internalized and accumulated mainly in the early endosomes [Herz and Strickland, 2001]. Finally, endocytosis and intracellular trafficking of LRP1 play a key role in regulating other plasma membrane receptors, such as the platelet-derived growth factor receptor β (PDGFRβ) [Boucher and Herz, 2011], the urokinase-plasminogen activator receptor (uPAR) [Gonias et al., 2011], membrane type 1-MMP (MT1-MMP) [Barcelona et al., 2013] and β1-integrin [Rabiej et al., 2016], thus controlling the cellular migration of normal and malignant cells.

Both α_2M and LRP1 play important roles in inflammatory processes by controlling the extracellular activity of several proteases, cytokines and growth factors [Chu and Pizzo, 1994]. Moreover, the binding of α_2M* to LRP1 can also activate the ERK/MAPK signaling pathway and the nuclear transcription factor, NF-κB, in macrophages, thereby inducing MMP-9 activation and cellular proliferation [Bonacci et al., 2007; Caceres et al., 2010]. Similarly, the α_2M*/LRP1 interaction promotes the glial fibrillary acidic protein (GFAP) expression in the Müller glial cell line, MIO-M1, mediated by JAK/STAT pathway activation [Barcelona et al., 2011]. On the same cell line, we have established that α_2M* increased the LRP1 and MT1-MMP accumulation in early endosomes, followed by endocytic recycling and intracellular distribution of MT1-

MMP toward cellular protrusions, thus increasing the cellular motility of these glial cells [Barcelona et al., 2013].

In general, distinct modes of migration contribute to diverse types of cell movements, ranging from the movement of single cells to collective cell migration [Friedl and Wolf, 2009]. The movement of individual cells is described as either "amoeboid" or "mesenchymal". Amoeboid migration is characterized by gliding and rapid migration; these cells exert relatively weak integrin-mediated traction forces on the surrounding substrate and can even be integrin-independent [Friedl and Wolf, 2009]. Mesenchymal cell migration is characterized by single cell motility and a multistep cycle of membrane protrusion, formation of focal cell adhesion, and stabilization at the leading edge followed by cell body contraction, focal adhesion release and rear detachment [Huttenlocher and Horwitz, 2011]. Mesenchymal migration in three-dimensional tissues is associated with the degradation of ECM and a regulated extracellular proteolysis. This mode of cellular migration is characteristic of fibroblasts, macrophages, and tumor cells, and it is directly associated with several inflammatory disorders and cancer [Frittoli et al., 2011].

Against this background, we hypothesize that, besides LRP1 intracellular signaling and endocytosis, α_2M* also induces the cellular migration of macrophages, which in turn could regulate the function of other membrane proteins involved in cellular adhesion and migration, such as MT1-MMP and β1-integrin. Thus, in the present work we investigate whether the α_2M*/LRP1 interaction induces cellular migration of the macrophage-derived cell line, Raw264.7.

MATERIALS AND METHODS

Cell cultures and reagents. Mouse Raw264.7 macrophage-derived cells were cultured in DMEM high glucose medium supplemented with 10% fetal bovine serum (FBS), penicillin (50 U/ml), and streptomycin (50 mg/ml) at 5% CO2, 95% humidity, and 37 °C. Alpha$_2$M was purified from human plasma following a procedure described previously [Chiabrando et al., 1997]. The activated form of α_2M (α_2M*) was generated by incubating purified α_2M with 200mM methylamine–HCl for 6 h at pH 8.2, as previously reported [Chiabrando et al., 2002]. An expression construct encoding RAP as a glutathione S-transferase (GST) fusion protein (GST-RAP) was kindly provided by Dr. Guojum Bu (Washington University, St. Louis, MO). GST-RAP was expressed and purified as described elsewhere [Bu et al., 1995] and used without further modification. In this work, 400 nM GST-RAP was used to inhibit the binding of α_2M* to LRP1, whereas we previously demonstrated that the use of GST (400 mM) alone has no inhibitory effects [Sanchez et al., 2001]. Immunofluorescences were performed with the following primary antibodies: mouse monoclonal anti-β subunit of LRP1 (clone 5A6); rabbit monoclonal anti-β subunit of LRP1 (EPR3724); mouse monoclonal anti-MT1-MMP; mouse monoclonal anti-phosphorylated FAK; mouse monoclonal anti-FAK; rabbit polyclonal anti-GM130; and rabbit monoclonal anti-β1-integrin, all of which were purchased from Abcam (Cambridge, MA, USA). Alexa Fluor-594- or 488-conjugated phalloidin, as well as secondary antibodies raised in goat anti-rabbit IgG conjugated with Alexa Fluor 647, 594 or 488 and anti-mouse IgG conjugated with Alexa Fluor 594 or 488 were from Invitrogen (Buenos Aires, Argentina). Calphostin-C (PKC inhibitor) was obtained from Sigma–Aldrich (St. Louis, MO), prepared as a stock solution (1 mM) in dimethyl sulfoxide (DMSO) and diluted to a final concentration of 100 μM with DMEM; with this dilution the DMSO proportion did not affect cell viability (data not shown).

Cell migration assays. Cell migration activities were examined by a two-dimensional wound-scratch assay in six-well plates coated with collagen type I (10 μg/cm^2; Sigma-Aldrich). Raw264.7 cells (5x10^5 cells/well) were cultured for 48 h at 37°C in DMEM-high glucose containing 10% FBS with 5% CO2, followed by overnight serum depletion. In each well, a straight lesion was created in the center of the Raw264.7 cell monolayer with a sterile 10-μl pipette tip. This technique produced a consistent wound devoid of cells, ≈35 mm long x 400 μm wide. The wells were then rinsed twice with serum-free medium to remove any cell debris and 2 ml of DMEM-high glucose without red phenol was added. Cells were treated with 60 nM α_2M* for 12 h. To block α_2M*/LRP1 binding, cells were previously treated with 400 nM GST-RAP for 30 min, and then the α_2M* stimulation step was performed in the presence of 400 nM GST-RAP. Cellular migration was measured following the procedure described previously [Liang et al., 2007]. Briefly, at selected times (0 and 12 h), three random images of the wound per condition were acquired using a charge-coupled device (CCD) camera (Nikon) on a bright-field microscope (Nikon TU-2000 inverted microscope; Nikon, Tokyo, Japan) with a X10 objective (0.3 NA). Each image defined an average area of the wound equivalent to 5x10^5±1x10^4 μm^2 recorded to t=0 h. Cells invading this area were counted to t=12 h and results were expressed as cells per area.

Confocal microscopy. To visualize the protein cellular localization, Raw264.7 cells were grown on glass coverslips coated with collagen type I (10 μg/cm^2) before being stimulated or not with α_2M* (60 nM) for 1 h. These cells were washed with PBS 1X, fixed with 4% paraformaldehyde, and incubated with a quenching solution (50 mM NH_4Cl). The cells were then permeabilized with 0.1% (v/v) Triton X-100, blocked with 2% BSA, and incubated with the respective primary antibody (diluted from 1/50 to 1/200) followed by incubation with a secondary antibody conjugated with Alexa Fluor

(diluted 1/800). For actin polymerization, cells were incubated with Alexa Fluor 594- or 488-phalloidin (diluted 1/150). Finally, they were washed with PBS 1X and mounted on glass slides with Mowiol 4–88 reagent from Calbiochem (Merck KGaA, Darmstadt, Germany). To evaluate the colocalization between different proteins and LRP1, fluorescent images were obtained with an Olympus FluoView FV300 or Olympus FluoView FV1000 confocal laser scanning biological microscope (Olympus, New York, NY, USA). Whole cells were scanned, and optical sections were gathered in 0.25-μm steps perpendicular to the z axis. Lastly, images were processed using FV10-ASW Viewer 3.1 (Olympus) and ImageJ software.

Statistical treatment of data. For cellular migration assays, results are expressed as mean ± standard error of mean (S.E.M) of independent experiments; a one-way ANOVA was used for comparisons. Differences from the control were considered significant at $p < 0.05$. For microscope quantifications of the level of colocalization, a JACoP plug-in from ImageJ software was used [Bolte and Cordelieres, 2006]. At least 50 cells/condition were analyzed. Then, the averages of the vesicle percentages containing both proteins were calculated from the Manders' coefficients and compared using the Student's t-test. Values of $p < 0.05$ were considered significant.

RESULTS

The α_2M*/LRP1 interaction induces intracellular signaling activation, MMP-9 expression and cellular proliferation in macrophages [Bonacci et al., 2007; Caceres et al., 2010]. However, the effect of α_2M* on macrophage migration has been poorly explored. A macrophage-derived cell line, Raw264.7, was thus cultured in the presence of α_2M* (60 nM) for 12 h at 37 °C on collagen type-I-coated plates, and the cellular migration was evaluated using a wound-scratch migration assay. Figure 1 shows

representative images (panel A) and the quantitative analysis (panel B) of cell migration assays which demonstrate that α_2M* induced a significant single cellular migration of Raw264.7 cells compared with the control condition (vehicle cell culture medium without α_2M*). This single migratory effect induced by α_2M* was abrogated by the presence of GST-RAP (400 nM), an inhibitor of the ligand-LRP1 binding. On the other hand, GST-RAP alone had no effect on cell motility, denoting that the migratory effect is induced by the α_2M*/LRP1 interaction. Moreover, α_2M*-stimulated cells invading the area of the wound revealed the formation of cellular protrusions (Figure 1, insets). By contrast, cells invading the wound area that were pretreated with GST-RAP or non-stimulated with α_2M* showed no evident development of cellular protrusions. These data suggest that α_2M*, mediated by its LRP1 interaction, induces a mesenchymal mode of cellular migration in Raw264.7 cells.

Many extracellular proteases expressed in mammalian cells, including matrix metalloproteases (MMPs), play a pivotal role in determining cell migratory processes by degrading ECM [Frittoli et al., 2011]. The subcellular localization and polarized distribution of MT1-MMP at the plasma membrane are key events for cellular migration with mesenchymal mode [Strongin, 2010]. In addition, we have previously reported that the α_2M*/LRP1 interaction can induce the MT1-MMP sorting to the plasma membrane, promoting the cellular motility of Müller glial cells [Barcelona et al., 2013]. Considering these antecedents, we examine the α_2M* effect on the cellular distribution of MT1-MMP in Raw264.7 cells by immunostaining and confocal microscopy. Figure 2 and Supplementary Figure S1 illustrate that the MT1-MMP showed a punctate perinuclear distribution under non-stimulated conditions; under α_2M* stimulation (60 nM for 1 h), though, MT1-MMP was peripherally distributed in structural vesicles

localized in cellular protrusions. In addition, LRP1 also showed punctate perinuclear distributions under non-stimulated conditions, and this receptor was evidently distributed to cellular protrusions under α_2M* stimulation. Finally, visualization and quantification of colocalization between MT1-MMP and LRP1 were not significant under α_2M* stimulation with respect to the control (10±2% vs. 9±2%; p>0.05). Thus, these results suggest that α_2M* induces the MT1-MMP and LRP1 traffic to cellular protrusions through different intracellular routes in Raw264.7 cells. Moreover, these cellular distributions of LRP1 and MT1-MMP induced by α_2M* was selective for these membrane proteins, because GM130 (a specific marker of Golgi network) was unaffected by the α_2M* stimulus with respect to non-stimulated cells (Supplementary Figure S2). Finally, treatment of Raw264.7 cells with cycloheximide did not abrogate cellular distributions of MT1-MMP and LRP1, indicating that this trafficking to cellular protrusions is not attributable to protein synthesis under the α_2M* stimulus (data not shown).

During cellular migration with the mesenchymal mode, cells adopt a motility type characterized by cytoskeleton remodeling with actin polymerization (F-actin) in elongated cell protrusions [Frittoli et al., 2011]. Considering these data, we examine LRP1 and F-actin in α_2M*-stimulated Raw264.7 cells by using LRP1 immunostaning and AlexaFluor 488-conjugated phalloidin, and then they were visualized by confocal microscopy. Figure 3 and Supplementary Figure S3 exhibit representative images where F-actin presented a peripheral cell surface distribution in α_2M*-untreated cells, together with punctuate perinuclear distribution of LRP1. Under α_2M* stimulation (60 nM for 1 hour), F-actin is detected in cellular protrusions, denoting that cytoskeleton remodeling is underway. In addition, merge images show that the α_2M*-induced LRP1 distribution

to cellular protrusions were not colocalized with actin polymerization sites. Furthermore, the quantitative analysis of α_2M*-induced cellular protrusions demonstrate that ≈80% of Raw264.7 cells undergo these events (Figure 3, bar graphs), which were significantly abrogated by the presence of GST-RAP. In previous studies we proved that the α_2M*/LRP1 interaction implied PKC activation and intracellular calcium mobilization in J774 and Raw264.7 macrophage-derived cells [Caceres et al., 2010], and considering that PKC is involved in cytoskeleton remodeling during cellular motility [Friedl and Wolf, 2009], we examine herein the effect of calphostin-C, a broad PKC inhibitor, on the formation of cellular protrusions induced by α_2M* stimulation in Raw264.7 cells. Figure 3 clearly exhibits that α_2M*-induced cellular protrusions were fully blocked by calphostin-C, thereby revealing that PKC activation is involved in the formation of this membrane event. Calphostin-C thus also inhibited the α_2M*-induced cellular migration of Raw264.7 cells (data not shown).

Integrins regulate cell migration as well as other cellular functions by coupling with multiple cytoskeletal and signaling molecules, many of which co-cluster with integrins at focal adhesions in adherent cells [Huttenlocher and Horwitz, 2011]. Focal adhesion kinase (FAK), a non-receptor tyrosine kinase, is one of the most prominent signaling molecules among these proteins [Huttenlocher and Horwitz, 2011; Zhao and Guan, 2011]. Hence, we hypothesize that the α_2M*/LRP1 interaction could induce cellular protrusions associated with an increased phosphorylation of FAK at this point of cell adhesion. Raw264.7 cells were thus stimulated with α_2M* (60 nM for 1 h) and the phosphorylated FAK (p-FAK) was examined by immunostaining together with LRP1 and F-actin. Figure 4 illustrates that p-FAK was detected in cellular protrusions of α_2M*-stimulated Raw264.7 cells, which reveals that focal adhesions occur in the same

region where the leading edge of cellular migration is taking place. On the other hand, p-FAK was distributed in multiple and perinuclear focal adhesions in α_2M* non-stimulated cells, which may be associated with high adherence and low motility under this condition. Moreover, the merge images show a low colocalization level between LRP1 and p-FAK at focal adhesion sites, which remains unchanged after α_2M* stimulation (10±2% vs. 11±2%; p>0.05). Like p-FAK distribution, the constitutive protein FAK was immunodetected at cellular protrusion regions in Raw264.7 cells stimulated with α_2M* (Supplementary Figure S4).

Previous reports have demonstrated that LRP1 interacts with β1-integrin [Lillis et al., 2005; Ranganathan et al., 2011] and, through LRP1 endocytosis, it regulates integrin internalization, cell surface activity and intracellular signaling [Rabiej et al., 2016]. However, the α_2M* effect on this intracellular LRP1/β1-integrin function has not been established. Therefore, we hypothesize that LRP1 endocytosis induced by α_2M* could influence β1-integrin internalization and promote cell migration. In this way, Raw264.7 cells were cultured in the presence of α_2M* (60 nM for 1 h) and the colocalization level of LRP1 and β1-integrin was analyzed by confocal microscopy. Figure 5-A shows that LRP1 and β1-integrin presented a very similar punctuate distribution both at the perinuclear region in α_2M*-non stimulated cells and at cellular protrusion in α_2M*-stimulated cells. However, the colocalization analysis between LRP1 and β1-integrin (Figure 5-B) reveals that α_2M* stimulation increased the mean percentage of colocalization with respect to non-stimulated cells (55±5% vs. 10±2%; p<0.05). Moreover, when the colocalization analysis was calculated at the perinuclear versus protrusion regions in α_2M*-stimulated cells (Figure 5-C), a higher percentage was obtained at protrusion with respect to perinuclear regions (58±6% vs. 38±4%; p<0.05).

Finally, these levels of colocalization between LRP1 and β1-integrin strongly diminished when cells were incubated with GST-RAP prior to α_2M* stimulus (10±2% vs. 12±3%; $p>0.05$), thereby indicating that the intracellular LRP1/β1-integrin association is induced by the α_2M*/LRP1 interaction in Raw264.7 cells.

DISCUSSION

It is well established that α_2M and LRP1 are involved in inflammatory processes by their ability to control several extracellular proteases and pro-inflammatory factors contributing to the cellular proliferation and migration of the innate immunity, in particular macrophages [Chu et al., 1994; Chu and Pizzo, 1994; Gaultier et al., 2008; Ranganathan et al., 2011]. In addition, LRP1 is highly expressed in macrophages during chronic inflammatory disorders, such as atherosclerosis [Boucher and Herz, 2011; Costales et al., 2013]. In macrophages, the α_2M*/LRP1 interaction induces intracellular signaling activation, which has been associated with intracellular calcium mobilization, cellular proliferation and MMP-9 expression [Caceres et al., 2010]. In the present study, we have demonstrated that the α_2M*/LRP1 interaction can also induce macrophage migration with a mesenchymal mode, which is mainly characterized by cellular enlarged protrusions, MT1-MMP and LRP1 distribution to these leading edge protrusions, actin polymerization, focal adhesion formation and increased intracellular LRP1/β1-integrin colocalization.

Several MMPs, principally MMP-9, MMP-2, and MT1-MMP have been involved in the cellular migration of normal and malignant cells [Strongin, 2010]. We have previously demonstrated that α_2M* induced cell migration and pro-MMP-2 activation in a human Müller glial cell line, MIO-M1, which was mediated by an increased LRP1 and MT1-MMP accumulation in early endosomes, followed by endocytic recycling and

intracellular distribution of MT1-MMP toward cellular protrusions [Barcelona et al., 2013]. In Raw264.7 cells α_2M* also induced a distribution of MT1-MMP and LRP1 to cellular protrusions, but molecular colocalization between both membrane proteins was not observed in endosome vesicles, suggesting that MT1-MMP trafficking to the plasma membrane in macrophages does not involve a direct molecular association with LRP1. Another difference is that α_2M* induces the synthesis of MMP-9 but not MMP-2 in macrophages [Caceres et al., 2010], whereas α_2M* promotes the activation of pro-MMP-2 without affecting the production of MMP-9 in glial cells [Barcelona et al., 2013]. It has been demonstrated that MMP-9 plays a key role in ECM remodeling during inflammatory processes and cancer, which promotes cellular migration through the contact of the surface cell with modified components of ECM [Song et al., 2009]. In this way, MT1-MMP can be trafficked to the plasma membrane by an exocytic route from biosynthetic storage compartments, which is induced by cell-MEC contact [Bravo-Cordero et al., 2007]. However, additional studies are needed in order to evaluate the α_2M* effect on the MT1-MMP function in Raw264.7 cells.

Cell migration requires the dynamic interaction between a cell and the substratum on which it is attached and over which it migrates. Distinct modes of migration contribute to diverse types of cell movements; they range from the movement of single cells to collective cell migration [Friedl and Wolf, 2009]. In the present study, we demonstrated that α_2M* increases the single motility of Raw264.7 cells with evident formation of cellular protrusions. This type of migration, also termed mesenchymal cell migration, is generally characterized by a multistep cycle of protrusions, formation of cell adhesions, and stabilization at the leading edge, which is associated with degradation of ECM and regulation of the extracellular proteolysis [Huttenlocher and Horwitz, 2011]. At the leading edge of cell protrusions, dynamic events of adhesions mediated by different

intracellular signaling pathways occur, including Rho GTPases, PI3 kinase, PTEN and PKC activation, which lead to the actin polymerization at lamellipodium [Friedl and Wolf, 2010]. We observed in this study that α_2M* promotes actin polymerization at cellular protrusions, which was abrogated by RAP and calphostin C, indicating that it is mediated by LRP1 and PKC activation. Previous reports have shown that the α_2M*/LRP1 interaction can activate intracellular signaling in macrophages, including PKC activation [Caceres et al., 2010], which suggests that this signaling pathway can mediate the cytoskeleton remodeling during the cell motility induced by α_2M*.

Integrins are transmembrane proteins with the ability of assembling to heterodimeric cell adhesion receptors involved in cell migration, cell adhesion and tumor development [Hynes, 2002]. Binding of integrins to ECM induces a conformational change to active integrin and thus connects the cytoskeleton to the ECM, whereby signal can be transduced either outside-in or inside-out [Huttenlocher and Horwitz, 2011]. In migrating cells, the binding of integrins to ECM proteins results in focal adhesion assembly at the leading edge, a process involving β1-integrin endocytosis in a clathrin-dependent manner [Chao and Kunz, 2009]. Our study shows that α_2M* induces focal adhesions in cellular protrusions of Raw264.7 cells with activation of FAK, one of the signaling and adaptor protein of the large complexes linked to actin cytoskeleton, which plays a key role in cell-matrix adhesion processes [Friedl and Wolf, 2010]. However, the absence of molecular localization between FAK and LRP1 in this focal adhesion sites suggest that LRP1 is not involved in the molecular complexes directly associated with focal adhesions.

A recent report has demonstrated that LRP1 endocytosis is a regulator of β1-integrin endocytosis and endocytic recycling in MEF cells, which involves β1-integrin

interaction with the distal NPxY motif of the LRP1 β-subunit, followed by LRP1-β1-integrin internalization through a clathrin-mediated endocytosis [Rabiej et al., 2016]. Our study demonstrates that α_2M* increases localization between LRP1 and β1-integrin in endosome vesicles distributed in cell perinuclear and protrusion regions, which suggests that α_2M* induces higher activity of endocytosis and endocytic recycling of β1-integrin mediated by an increased internalization of LRP1. We have previously shown the ability of the α_2M*/LRP1 interaction to regulate the expression and function of MT1-MMP, which play a key role in the cellular migration of Muller glial cells [Barcelona et al., 2013; Gonias et al., 2011]. Thus, α_2M* can act as an inductor of these migratory processes mediated by its interaction with LRP1 in different types of cells, which may be related with several disorders, such as retinal neurodegeneration, chronic inflammation and cancer. It is hence known that blood native α_2M undergoes extravasation to interstitial spaces during these disorders and interacts with proteases delivered in these altered sites, forming α_2M-protease complexes or α_2M* [Chu and Pizzo, 1994]. This α_2M* acquires the ability to recognize LRP1 and from its interaction down-stream it activates intracellular signaling, cell motility, cellular proliferation and MMP activation [Bonacci et al., 2007; Caceres et al., 2010]. These findings taken together could constitute a therapeutic target for inflammatory processes, such as rheumatoid arthritis and atherosclerosis, and cancer.

ACKNOWLEDGMENTS

The authors wish to thank Gabriela Diaz Cortez for her language assistance as well as Dr. Pilar Crespo, Dr. Cecilia Sampedro and Dr. Carlos Mas (Technical Support Professionals, CONICET) for the microscope technical assistance. D.G.F. is a doctoral

fellow at CONICET. V.A-D. is a doctoral fellow at FONCyT, M.C.S. and G.A.C. are members of the Research Career of CONICET.

REFERENCES

Barcelona PF, Jaldin-Fincati JR, Sanchez MC, Chiabrando GA. 2013. Activated alpha2-macroglobulin induces Muller glial cell migration by regulating MT1-MMP activity through LRP1. FASEB J 27:3181-97.

Barcelona PF, Ortiz SG, Chiabrando GA, Sanchez MC. 2011. alpha2-Macroglobulin induces glial fibrillary acidic protein expression mediated by low-density lipoprotein receptor-related protein 1 in Muller cells. Invest Ophthalmol Vis Sci 52:778-86.

Bolte S, Cordelieres FP. 2006. A guided tour into subcellular colocalization analysis in light microscopy. J Microsc 224:213-32.

Bonacci GR, Caceres LC, Sanchez MC, Chiabrando GA. 2007. Activated alpha(2)-macroglobulin induces cell proliferation and mitogen-activated protein kinase activation by LRP-1 in the J774 macrophage-derived cell line. Arch Biochem Biophys 460:100-6.

Boucher P, Herz J. 2011. Signaling through LRP1: Protection from atherosclerosis and beyond. Biochem Pharmacol 81:1-5.

Bravo-Cordero JJ, Marrero-Diaz R, Megias D, Genis L, Garcia-Grande A, Garcia MA, Arroyo AG, Montoya MC. 2007. MT1-MMP proinvasive activity is regulated by a novel Rab8-dependent exocytic pathway. EMBO J 26:1499-510.

Bu G, Geuze HJ, Strous GJ, Schwartz AL. 1995. 39 kDa receptor-associated protein is an ER resident protein and molecular chaperone for LDL receptor-related protein. EMBO J 14:2269-80.

Caceres LC, Bonacci GR, Sanchez MC, Chiabrando GA. 2010. Activated alpha(2) macroglobulin induces matrix metalloproteinase 9 expression by low-density lipoprotein receptor-related protein 1 through MAPK-ERK1/2 and NF-kappaB activation in macrophage-derived cell lines. J Cell Biochem 111:607-17.

Chao WT, Kunz J. 2009. Focal adhesion disassembly requires clathrin-dependent endocytosis of integrins. FEBS Lett 583:1337-43.

Chiabrando G, Bonacci G, Sanchez C, Ramos A, Zalazar F, Vides MA. 1997. A procedure for human pregnancy zone protein (and human alpha 2-macroglobulin) purification using hydrophobic interaction chromatography on phenyl-sepharose CL-4B column. Protein Expr Purif 9:399-406.

Chiabrando GA, Sanchez MC, Skornicka EL, Koo PH. 2002. Low-density lipoprotein receptor-related protein mediates in PC12 cell cultures the inhibition of nerve growth factor-promoted neurite outgrowth by pregnancy zone protein and alpha2-macroglobulin. J Neurosci Res 70:57-64.

Chu CT, Howard GC, Misra UK, Pizzo SV. 1994. Alpha 2-macroglobulin: a sensor for proteolysis. Ann N Y Acad Sci 737:291-307.

Chu CT, Pizzo SV. 1994. alpha 2-Macroglobulin, complement, and biologic defense: antigens, growth factors, microbial proteases, and receptor ligation. Lab Invest 71:792-812.

Costales P, Castellano J, Revuelta-Lopez E, Cal R, Aledo R, Llampayas O, Nasarre L, Juarez C, Badimon L, Llorente-Cortes V. 2013. Lipopolysaccharide downregulates CD91/low-density lipoprotein receptor-related protein 1 expression through SREBP-1 overexpression in human macrophages. Atherosclerosis 227:79-88.

Friedl P, Wolf K. 2009. Proteolytic interstitial cell migration: a five-step process. Cancer Metastasis Rev 28:129-35.

Friedl P, Wolf K. 2010. Plasticity of cell migration: a multiscale tuning model. J Cell Biol 188:11-9.

Frittoli E, Palamidessi A, Disanza A, Scita G. 2011. Secretory and endo/exocytic trafficking in invadopodia formation: the MT1-MMP paradigm. Eur J Cell Biol 90:108-14.

Gaultier A, Arandjelovic S, Niessen S, Overton CD, Linton MF, Fazio S, Campana WM, Cravatt BF, 3rd, Gonias SL. 2008. Regulation of tumor necrosis factor receptor-1 and the IKK-NF-kappaB pathway by LDL receptor-related protein explains the antiinflammatory activity of this receptor. Blood 111:5316-25.

Gonias SL, Gaultier A, Jo M. 2011. Regulation of the urokinase receptor (uPAR) by LDL receptor-related protein-1 (LRP1). Curr Pharm Des 17:1962-9.

Herz J, Strickland DK. 2001. LRP: a multifunctional scavenger and signaling receptor. J Clin Invest 108:779-84.

Hussain MM, Strickland DK, Bakillah A. 1999. The mammalian low-density lipoprotein receptor family. Annu Rev Nutr 19:141-72.

Huttenlocher A, Horwitz AR. 2011. Integrins in cell migration. Cold Spring Harb Perspect Biol 3:a005074.

Hynes RO. 2002. Integrins: bidirectional, allosteric signaling machines. Cell 110:673-87.

Laatsch A, Panteli M, Sornsakrin M, Hoffzimmer B, Grewal T, Heeren J. 2012. Low density lipoprotein receptor-related protein 1 dependent endosomal trapping and recycling of apolipoprotein E. PLoS One 7:e29385.

Liang CC, Park AY, Guan JL. 2007. In vitro scratch assay: a convenient and inexpensive method for analysis of cell migration in vitro. Nat Protoc 2:329-33.

Lillis AP, Mikhailenko I, Strickland DK. 2005. Beyond endocytosis: LRP function in cell migration, proliferation and vascular permeability. J Thromb Haemost 3:1884-93.

Mantuano E, Henry K, Yamauchi T, Hiramatsu N, Yamauchi K, Orita S, Takahashi K, Lin JH, Gonias SL, Campana WM. 2011. The unfolded protein response is a major mechanism by which LRP1 regulates Schwann cell survival after injury. J Neurosci 31:13376-85.

Rabiej VK, Pflanzner T, Wagner T, Goetze K, Storck SE, Eble JA, Weggen S, Mueller-Klieser W, Pietrzik CU. 2016. Low density lipoprotein receptor-related protein 1 mediated endocytosis of beta1-integrin influences cell adhesion and cell migration. Exp Cell Res 340:102-15.

Ranganathan S, Cao C, Catania J, Migliorini M, Zhang L, Strickland DK. 2011. Molecular basis for the interaction of low density lipoprotein receptor-related protein 1 (LRP1) with integrin alphaMbeta2: identification of binding sites within alphaMbeta2 for LRP1. J Biol Chem 286:30535-41.

Ridley AJ, Schwartz MA, Burridge K, Firtel RA, Ginsberg MH, Borisy G, Parsons JT, Horwitz AR. 2003. Cell migration: integrating signals from front to back. Science 302:1704-9.

Sanchez MC, Chiabrando GA, Vides MA. 2001. Pregnancy zone protein-tissue-type plasminogen activator complexes bind to low-density lipoprotein receptor-related protein (LRP). Arch Biochem Biophys 389:218-22.

Song H, Li Y, Lee J, Schwartz AL, Bu G. 2009. Low-density lipoprotein receptor-related protein 1 promotes cancer cell migration and invasion by inducing the expression of matrix metalloproteinases 2 and 9. Cancer Res 69:879-86.

Strongin AY. 2010. Proteolytic and non-proteolytic roles of membrane type-1 matrix metalloproteinase in malignancy. Biochim Biophys Acta 1803:133-41.

Zhao X, Guan JL. 2011. Focal adhesion kinase and its signaling pathways in cell migration and angiogenesis. Adv Drug Deliv Rev 63:610-5.

LEGENDS

Figure 1: **α_2M* induces single Raw264.7 cell migration through LRP1.** Cells were cultured for 12 h in serum-free DMEM, in the absence or presence of α_2M* (60 nM). ***A)*** Wound-scratch assay of Raw264.7 cells cultured in plates coated with collagen type-I. For blocking the α_2M* binding to LRP1, cells were pre-treated with GST-RAP (400 nM) for 30 min and then incubated with α_2M* (60 nM) plus GST-RAP (400 nM) for 12 h. The overlaid images (Insets) are magnifications of cells invading the wound area (boxes) under each experimental condition. ***B)*** Mean values of the cell number invading the wound area (cells/area) in the absence (Control) or presence of α_2M* (60 nM); pre-treated with GST-RAP (400 nM) prior to stimulation or not with α_2M* (60 nM). The wound-scratch assay is detailed in Materials and Methods. Three independent experiments were performed in triplicate. Values are expressed as mean ± S.E.M. ***p** < 0.05 *vs*. control.

Figure 2: α_2M* induces intracellular distribution of LRP1 and MT1-MMP toward cellular protrusions. Confocal microscopy images of LRP1 and MT1-MMP in Raw264.7 cells treated with serum-free DMEM (Control) or α_2M* (60 nM) for 1 h. For the immunodetection procedure, a rabbit monoclonal antibody anti-β subunit of LRP1 (green) and a mouse monoclonal anti-MT1-MMP antibody (red) were used. The overlaid images (Inset) are magnifications of cellular regions for LRP1 and MT1-MMP colocalization (boxes). Details of confocal microscopy and experiments are reported in Materials and Methods. All results are representative of three independent experiments.

Figure 3: α_2M*/LRP1 interaction induces actin polymerization and cellular protrusions mediated by PKC activation. A) Confocal microscopy of the LRP1 immunodetection and F-actin detected by AlexaFluor 488-conjugated phalloidin (green) in Raw264.7 cells treated with serum-free DMEM (control) or α_2M* (60 nM) for 1 h. For the immunodetection procedure, a rabbit monoclonal anti-β subunit of LRP1 (red) was used. The overlaid images (Inset) are magnifications of cell regions for LRP1 and F-actin (boxes). For blocking the α_2M* binding to LRP1 or PKC inhibition, cells were pre-treated with GST-RAP (400 nM) or calphostin C (100 μM) for 30 min and then stimulated with α_2M* (60 nM) for 1 h. Scale bars =10 μm. **B**) Mean values of the percentage of cells with cellular protrusions (activated cells) in the absence (Control) or presence of α_2M* (60 nM), pre-treated with GST-RAP (400 nM) or calphostin C (100 μM). A cellular protrusion was defined as a projection of cell surface whose length exceeds at least once cell soma [Ridley et al., 2003]. Details of experiments are reported in Materials and Methods. Three independent experiments were performed in triplicate. Values are expressed as mean ± S.E.M. * $\boldsymbol{p} < 0.05$ *vs*. control.

Figure 4: α_2M* induces p-FAK activation to cellular protrusions. Confocal microscopy of p-FAK and LRP1 immunodetection as well as F-actin detected by AlexaFluor 594-conjugated phalloidin (red) in Raw264.7 cells treated with serum-free DMEM (Control) or α_2M* (60 nM) for 1 h. For the immunodetection procedure, a rabbit monoclonal anti-β subunit of LRP1 (green) and a mouse monoclonal anti-pFAK antibody (revealed with Alexa Fluor 647-conjugated secondary antibody - pseudocolor in blue) were used. The overlaid images (Insets) are magnifications of cell regions for p-

FAK (boxes). Scale bars =10 μm. Details of experiments are reported in Materials and Methods. Three independent experiments were performed in triplicate.

Figure 5: α_2M* increases intracellular colocalization between LRP1 and β1-integrin. A) Confocal microscopy of the LRP1 and β1-integrin immunodetection using specific monoclonal antibodies as well as F-actin detected by AlexaFluor 594-conjugated phalloidin (pseudocolor in blue) in Raw264.7 cells treated with serum-free DMEM (control) or α_2M* (60 nM) for 1 h. For the immunodetection procedure, a mouse monoclonal anti-β subunit of LRP1 (green) and a rabbit monoclonal anti-β1 integrin antibody (red) were used. The overlaid images (Inset) are magnifications of cell regions for LRP1, β1-integrin and phalloidin (boxes). Binary images (white structural vesicles) of LRP1 and β1-integrin colocalization are also shown. Scale bars =20 μm. **B**) Mean percentage of total colocalization between LRP1 and β1-integrin in the absence (control) and presence of α_2M* (60 nM). **C**) Mean percentage of colocalization between LRP1 and β1-integrin discriminated in cellular perinuclear and protrusion regions in the absence (control) and presence of α_2M* (60 nM). Details of confocal microscopy and experiments are reported in Materials and Methods. All results are representative of three independent experiments. Values are expressed as mean ± S.E.M. * $\boldsymbol{p} < 0.05$ *vs*. control.

LEGENDS OF SUPPLEMENTARY FIGURES

Supplementary Figure S1: α_2M* induces intracellular distribution of LRP1 and MT1-MMP toward cellular protrusions. Raw264.7 cells cultured in glass coverslips coated with collagen type I and then treated with serum-free DMEM (Control) or α_2M* (60 nM) for 1 h. Representative image of confocal microscopy for: **A) LRP1** immunodetection using a mouse monoclonal anti-β subunit of LRP1 revealed with Alexa Fluor 488-conjugated secondary antibody; and B) **MT1-MMP** immunodetection using a mouse monoclonal anti-β MT1-MMP revealed with Alexa Fluor 488-conjugated secondary antibody. In these experiments, each primary antibody was individually processed and non-combined between them. The overlaid images (Inset) are magnifications of cell regions for LRP1 and MT1-MMP colocalization analysis (boxes). Details of confocal microscopy and experiments are reported in Materials and Methods. All results are representative of three independent experiments.

Supplementary Figure S2: α_2M* induces intracellular distribution of LRP1, but not GM130, toward cellular protrusions. Confocal microscopy of the LRP1 and GM130 immunodetection as well as actin polymerization by AlexaFluor 594-conjugated phalloidin (red) in Raw264.7 cells cultured in glass coverslips coated with collagen type I and then treated with serum-free DMEM (control) or α_2M* (60 nM) for 1 h. For the immunodetection procedure, a mouse monoclonal anti-β subunit of LRP1 revealed with Alexa Fluor 488-conjugated secondary antibody (green) and a rabbit monoclonal anti-GM130 antibody revealed with Alexa Fluor 647-conjugated secondary antibody (pseudocolor in blue) were used. The overlaid images (Insets) are

magnifications of cell regions for LRP1 and GM130 (boxes). Details of confocal microscopy and experiments are reported in Materials and Methods.

Supplementary Figure S3: α_2M* induces actin polymerization and intracellular distribution of LRP1 toward cellular protrusions. Confocal microscopy of the LRP1 immunodetection and actin polymerization (F-actin) detected by AlexaFluor 488-conjugated phalloidin (green) in Raw264.7 cells cultured in glass coverslips coated with collagen type I and then treated with serum-free DMEM (control) or α_2M* (60 nM) for 1 h. For immunodetection a rabbit monoclonal anti-β subunit of LRP1 revealed with Alexa Fluor 594-conjugated secondary antibody (red) was used. The overlaid images (Inset) are magnifications of cell regions for LRP1 and F-actin (boxes). Details of experiments are described in Materials and Methods.

Supplementary Figure S4: α_2M* induces constitutive protein FAK distribution towards cellular protrusions in Raw264.7 cells. A) Confocal microscopy of FAK and LRP1 immunodetections as well as actin polymerization (F-actin) detected by AlexaFluor 594-conjugated phalloidin (red) in Raw264.7 cells cultured in glass coverslips coated with collagen type I and then treated with serum-free DMEM (control) or α_2M* (60 nM) for 1 h. The overlaid images (Insets) are magnifications of cell regions for LRP1, FAK and F-actin (boxes). For immunodetection, a rabbit monoclonal anti-β subunit of LRP1 revealed with Alexa Fluor 488–conjugated secondary antibody (green) and a mouse monoclonal anti-FAK antibody revealed with Alexa Fluor 647-conjugated secondary antibody (pseudocolor in blue) were used. Scale bars =10 μm. B) Mean values of the percentage of colocalization between LRP1 vs. F-actin and LRP1 vs. FAK in cellular protrusions in the absence (control) or presence of

α_2M* (60 nM). Details of experiments are reported in Materials and Methods. Three independent experiments were performed in triplicate.

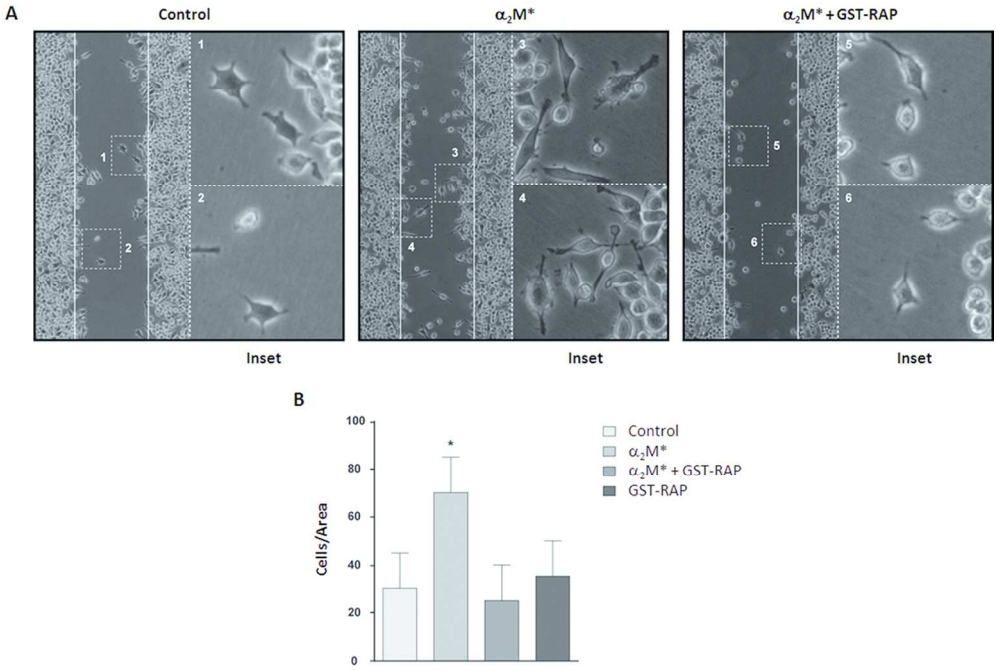

Figure 1

114x77mm (300 x 300 DPI)

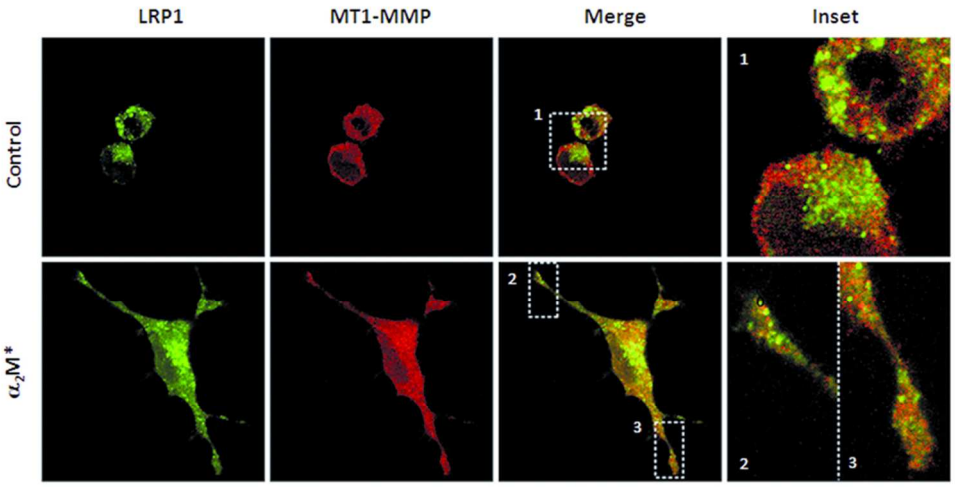

Figure 2

88x46mm (300 x 300 DPI)

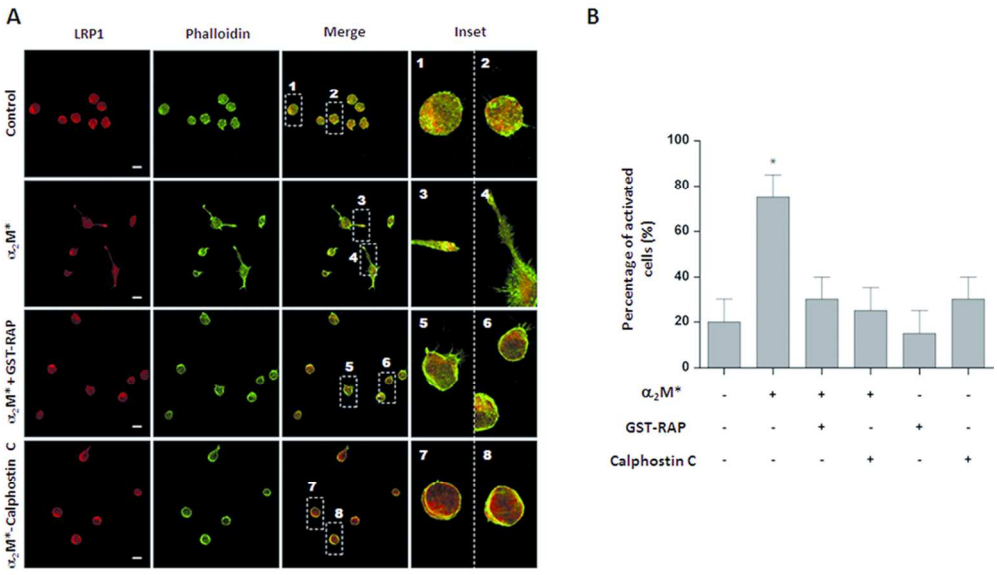

Figure 3

99x58mm (300 x 300 DPI)

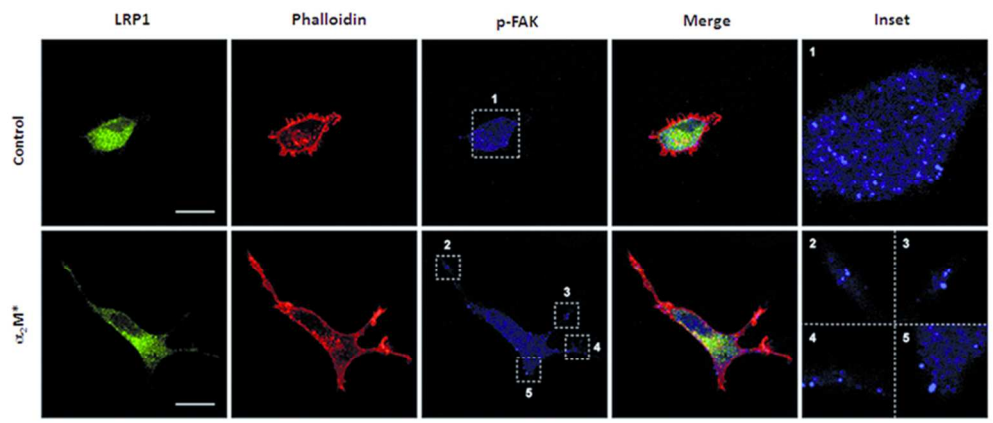

Figure 4

74x33mm (300 x 300 DPI)

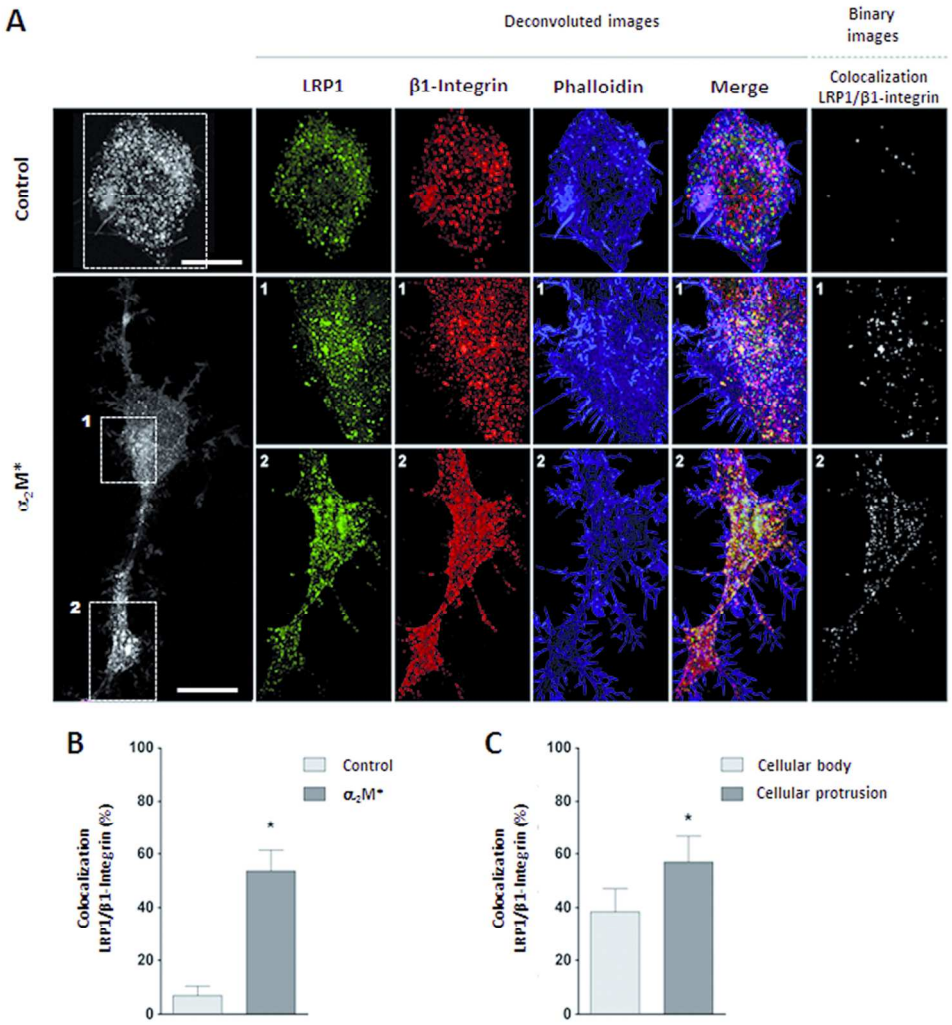

Figure 5

169x177mm (300 x 300 DPI)

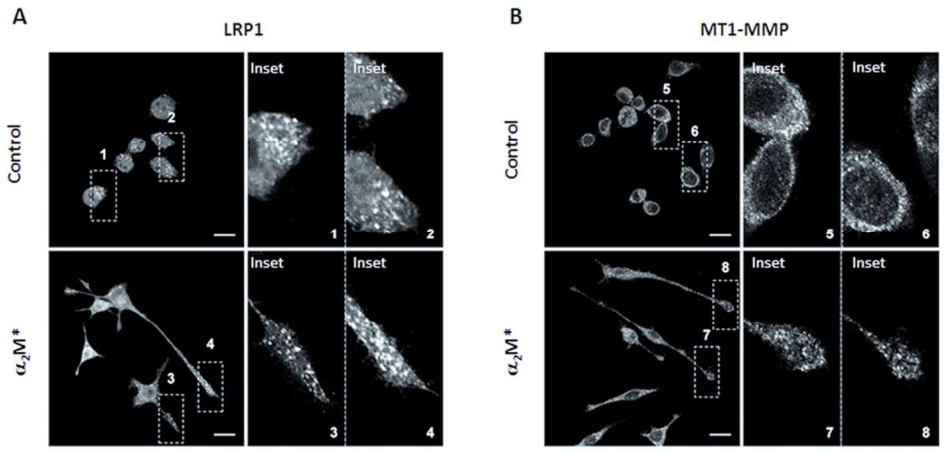

91x49mm (300 x 300 DPI)

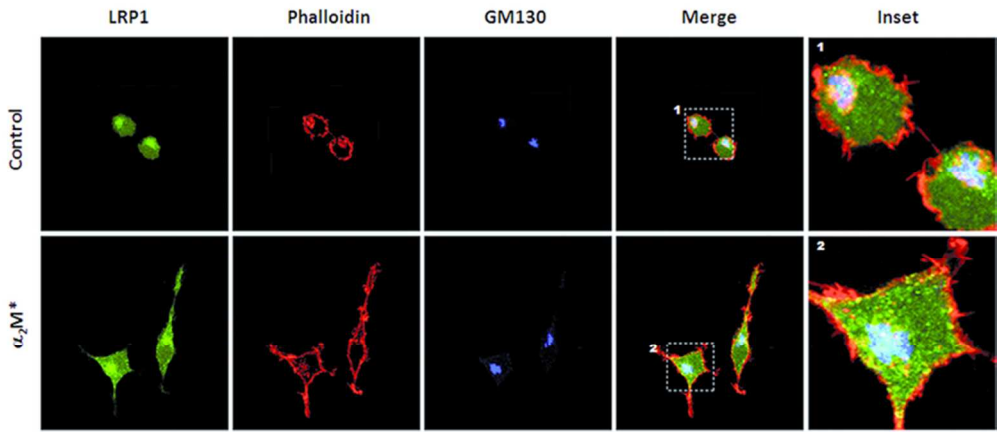

73x31mm (300 x 300 DPI)

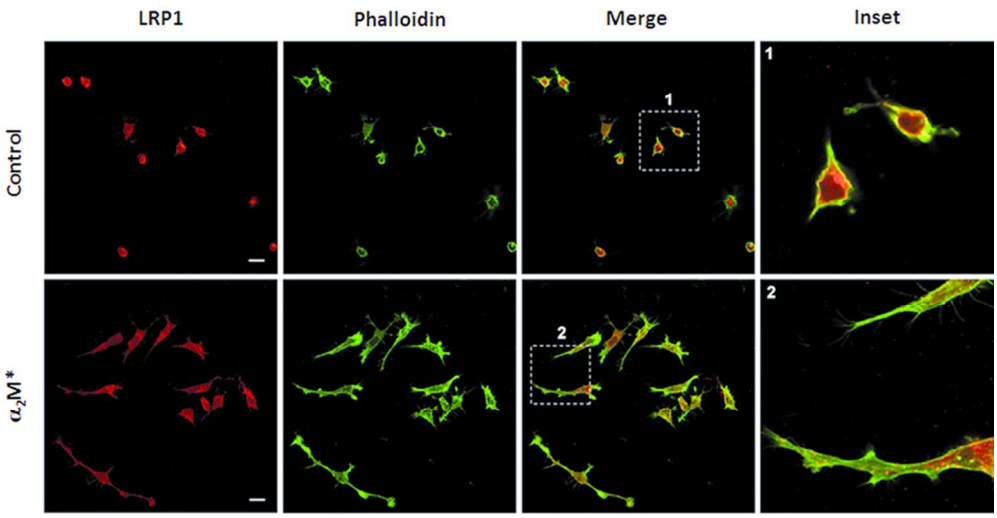

88x46mm (300 x 300 DPI)

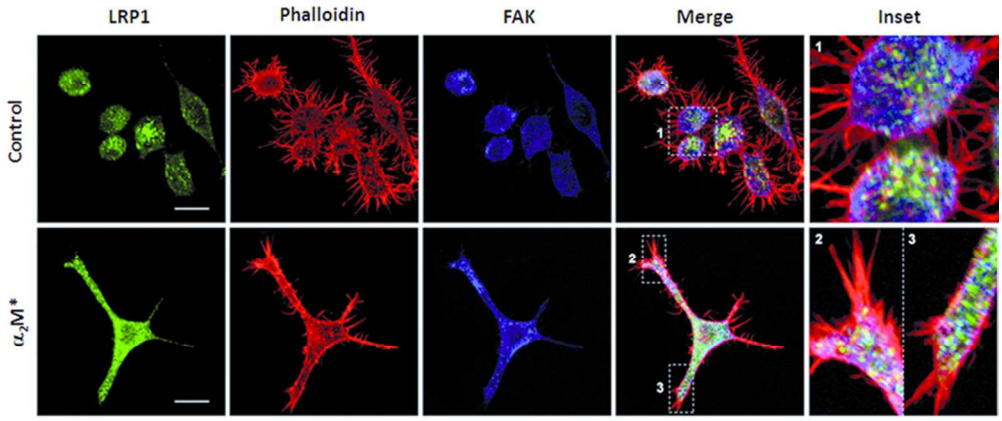

73x32mm (300 x 300 DPI)